IEEE Photonics Journal
An IEEE Photonics Society Publication

Open Access

Precise Fault Location in TDM-PON by Utilizing Chaotic Laser Subject to Optical Feedback

Volume 7, Number 6, December 2015

Tong Zhao
Hong Han
JianGuo Zhang
XiangLian Liu
XiaoMing Chang
AnBang Wang
YunCai Wang

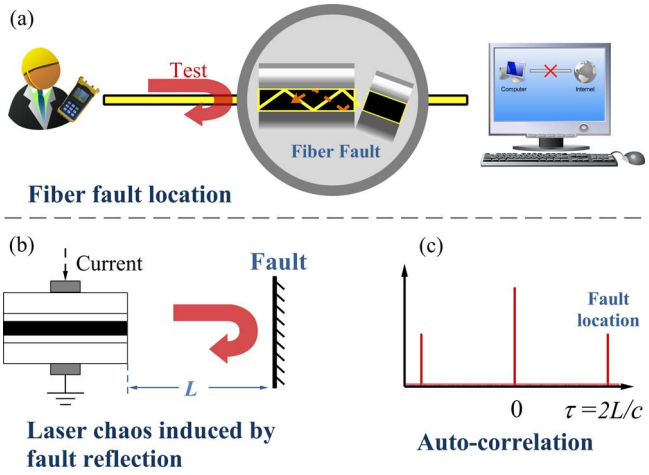

DOI: 10.1109/JPHOT.2015.2502258
1943-0655

IEEE photonics SOCIETY

IEEE

Precise Fault Location in TDM-PON by Utilizing Chaotic Laser Subject to Optical Feedback

Tong Zhao,[1,2] Hong Han,[1,2] JianGuo Zhang,[1,2] XiangLian Liu,[1,2] XiaoMing Chang,[2] AnBang Wang,[1,2] and YunCai Wang[1,2]

[1]Key Laboratory of Advanced Transducers and Intelligent Control System (Taiyuan University of Technology), Ministry of Education and Shanxi Province, Taiyuan 030024, China
[2]College of Physics and Optoelectronics, Taiyuan University of Technology, Taiyuan 030024, China

DOI: 10.1109/JPHOT.2015.2502258

Manuscript received October 13, 2015; accepted November 16, 2015. Date of publication November 19, 2015; date of current version November 30, 2015. This work was supported in part by the National Natural Science Foundation of China under Grant 61205142, Grant 61475111, and Grant 61475112; by the International Science and Technology Cooperation Program of China under Grant 2014DFA50870; by the Program for the Outstanding Innovative Teams of Information Security and Fault Detection in Communication Network; by the Key Program for Shanxi Innovative Research Team for Science and Technology under Grant 2013091021; and by the Program for the Innovative Talents of Higher Learning Institutions of Shanxi. Corresponding authors: A. Wang and Y. Wang (e-mail: wanganbang@tyut.edu.cn; wangyc@tyut.edu.cn).

Abstract: We propose a method with high spatial resolution to detect fiber faults in a time-division multiplexing passive optical network (TDM-PON). A semiconductor laser serving as the probe light source is subjected to self-feedback caused by reflection at fiber faults. The feedback will induce the laser to generate chaos. Autocorrelation of the output time series shows the external cavity signature and, therefore, indicates the distance between the laser and the fiber fault. Each branch is identified by the marker that is formed by the inserted fiber Bragg grating (FBG) providing the feedback in each branch, and the faulty branch can be distinguished by the marker that has disappeared. Our proof-of-concept experiment demonstrates the identification of the faulty branch and the location of the fault point in an optical network simultaneously. This is achieved with a 6-km feeder fiber and realizes the 8-mm spatial resolution.

Index Terms: Time-division multiplexed-passive optical network (TDM-PON), chaotic laser, fault location, optical feedback.

1. Introduction

The time-division multiplexed-passive optical network (TDM-PON) has been massively deployed in recent years since its point-to-multipoint network architecture has the best cost to performance ratio with high serial data-rate and a large capacity of transmission. To guarantee the quality of the communication service, a number of monitoring techniques have been developed [1]–[3].

In the TDM-PON, the optical light transmitted from the central office is equally distributed to each branch by a power splitter. The monitoring signal in each branch is the same and so cannot be distinguished. Therefore, growing attention has been given to devising a monitoring technique which will uniquely identify any faulty branch. The most direct approach is to actively select each branch fiber to examine at the splitter [4]–[11] or optical network units' (ONUs) area [12]–[17].

Another approach is to add some unique feature, which can be analyzed by the trace of the optical time-domain reflectometry (OTDR), to identify each branch, such as fiber length [18], wavelength [19]–[25] and code [26]–[28]. The third approach consists in analyzing the radio-frequency spectrum, where a different frequency is associated with each branch. The frequency feature can be generated by Brillouin frequency shifts of the fiber [29], the resonance frequency between laser and reflector [30], [31], and the cavity mode of the "self-injection locked reflective semiconductor optical amplifier" (SL-ROSA) [32], which replaces the laser in the ONU.

However, fault location problem remained an open issue for rapid maintenance. Some of the techniques mentioned above cannot realize fault location [1], and others locate the fault by utilizing OTDR. The principle of OTDR involves a tradeoff between spatial resolution and measurable range. Generally, the spatial resolution is about several meters [33] or worse when the fault occurs at a distance of tens of kilometers [34]. This resolution is not suitable for densely deployed fibers in an optical access network. Ultra-short pulse techniques can improve spatial resolution, but expensive devices and complicated techniques are required [35], [36].

Correlation OTDR [37] is proposed to overcome the above-mentioned tradeoff. By utilizing a pseudorandom or random code sequences to modulate the monitoring laser, the fault can be located via the cross-correlation function between the reference signal and the backscattered signal. To decrease the operational expenditure, the monitoring laser can be replaced by a communication laser modulated by a pseudorandom code; however, the superimposed code degrades the quality of the communication if the code is not filtered out [38]. Due to the expense of the high-speed code generator and the wideband modulator, the modulation method cannot significantly improve the spatial resolution. Regarding the traffic signal as a random modulated code, the in-service monitoring method has been proposed [39], [40], which, however, cannot be applied in TDM-PON, because of the indistinguishable broadcasting form in each branch. Recently, much research shows that the chaotic laser has a random intensity fluctuation and an ideal thumbtack ambiguity function [41]. Moreover, the broad bandwidth of the chaos [42]–[46] can compensate for the bandwidth limitation of the electronic component. It has been used for high spatial resolution ranging [47]–[50], even for the fault location in WDM-PON [51]. However, chaos detection has not been utilized in the TDM-PON monitoring.

In this work, we present a method with high spatial resolution for TDM-PON monitoring, utilizing a chaotic laser subject to optical feedback. The feedback is provided by the reflection of the fiber Bragg grating (FBG) or fault point. We demonstrate a proof-of-concept experiment and realize fault location together with branch identification.

2. Principle

A fiber fault can cause Fresnel reflection at the break surface because of the mismatching refractive indexes of the fiber and the surrounding air. In the technique of fault diagnosis, the operator must receive the fault information, accompanying the reflected test light, as shown in Fig. 1(a). By analyzing the original transmitted and reflected signals, the fault information can be acquired, e.g., in the OTDR technique, the distance relates to the round trip time of the pulse between the operator and the fault point; the received power relates to the attenuation of the fault. The test light in the fiber is usually emitted from a semiconductor laser. Without any other intervention in the transmission direction of the laser light, the reflection from the fault will directly feed back to the semiconductor laser. This is a typical structure for chaos generation.

As shown in Fig. 1(b), returning a fraction of the laser emission into the semiconductor laser will result in chaos output [52]–[54]. The mirror and laser cavity's surface consist of an external cavity with a cavity length L. The reflection of the fault may induce chaos in the monitoring laser where L is the distance from the laser to the fault.

With the extensive studies on chaotic lasers [55], [56], it has been shown that the length of the external cavity, known as the "external cavity signature," can be extracted from the output of the chaotic laser. This may be achieved using several methods, such as auto-correlation function (ACF), delay mutual information [57], [58], power spectrum analysis [59] or permutation

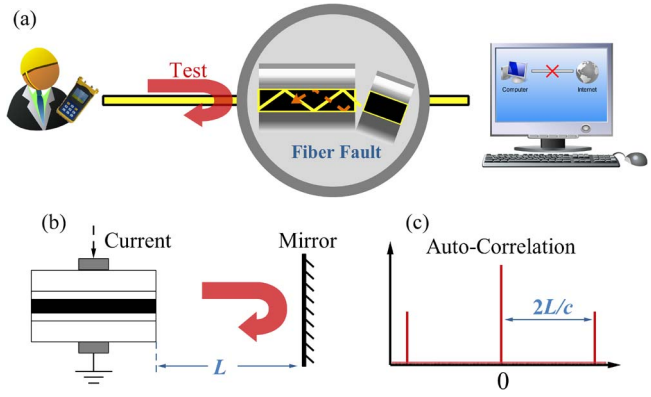

Fig. 1. Principle of the monitoring method. (a) Fault detection depends on the reflection information. (b) Typical chaos generation structure with optical feedback. (c) Autocorrelation of the chaotic laser subject to optical feedback.

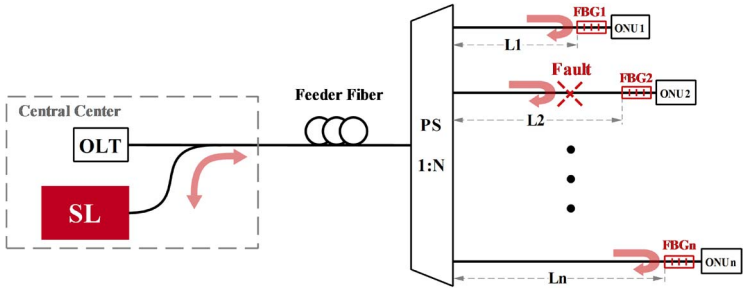

Fig. 2. Schematic of the monitoring technology in the TDM-PON utilizing external cavity signature of the chaos output of the semiconductor laser with optical feedback. Each FBG with a different fiber length is inserted into each branch to provide the optical feedback to the semiconductor laser, and the monitoring wavelength is nonintrusive with the communication wavelength. OLT: optical line terminal; PS: power splitter; ONU: optical network unit; SL: semiconductor laser; FBG: fiber Bragg grating; L: distance between PS and FBG.

entropy [60]. Here, we use the ACF method to extract the signature. Fig. 1(c) shows the ACF of the chaotic laser subject to optical feedback. Except for the main peak, there are two symmetrical side-lobes corresponding to the signature at the position of $\pm 2L/c$, where c is the speed of light. According to this relationship, the length of the external cavity is acquired. However, the existence of this signature is recognized as a nuisance in previous chaos applications, because it corresponds to a periodicity of the chaotic laser in contrast to the random oscillating property. More recently, researchers proposed many complicated feedback mechanisms or restricted feedback conditions to suppress or conceal this signature [44], [57], [61]–[66]. This indicates the difficulty of the elimination of this signature in the typical simple feedback structure. Therefore, the reflection of the fault can perturb the semiconductor laser to generate chaos and the fault position can be located via the external cavity signature.

3. Method and Experimental Results

Fig. 2 shows the schematic of our proposed monitoring method for the TDM-PON. In the TDM-PON, an optical line terminal is linked to the optical network units (ONUs) by a feeder fiber, a power splitter, and branch fibers. A semiconductor laser without an inbuilt isolator is used as the monitoring light source. In each branch, a FBG is inserted close to the ONU. The FBG has the same central wavelength with the probe laser and can then reflect the laser light back. The ACF can be calculated in the central office utilizing a small part of the laser light after being converted into an electrical signal by a photodetector.

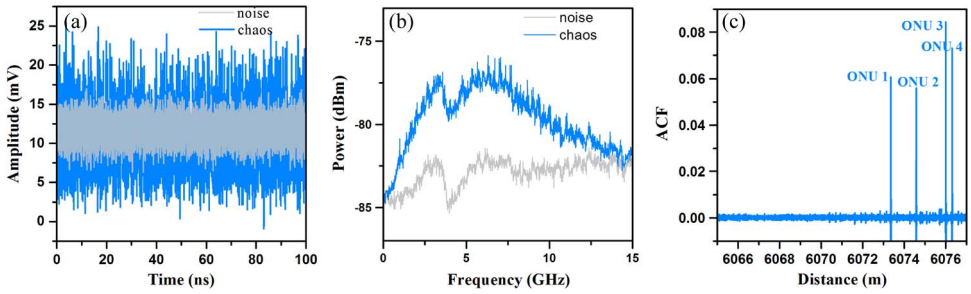

Fig. 3. Property of the chaotic laser generated by optical feedback from the reflector in each branch when our experiment PON is healthy. (a) Time series and (b) power spectrum of the laser with (blue) and without (gray) feedback. (c) Autocorrelation of the chaotic laser.

If all fibers in the TDM-PON are healthy, the corresponding FBG serves as an external reflector and induces chaos in the laser. Consequently, the position of this FBG can be read by the external cavity signature. Therefore, the location of the FBG is used as a mark to identify the branch fiber. If a branch fiber has a breakpoint, the feedback from the characteristic grating greatly reduces or disappears and a new feedback rises from the fault. Consequently, the signature of the FBG disappears and a new signature appears corresponding to the position where the breakpoint occurs. According to this change in signature, the broken branch fiber and the position of the breakpoint can be identified. It is worth noting that the wavelength of the probe laser can be chosen to be different from the communication wavelength in the TDM-PON to avoid interference. Furthermore the monitoring laser light can be coupled into the feeder fiber utilizing a wavelength division multiplexor. In addition, the FBGs' bandwidth should be larger than the linewidth of the probe laser in a chaotic state so that the FBGs act as a mirror reflection and then yield a strong cavity signature to mark the branches clearly.

In our proof-of-concept experiment, we use a 1×4 power splitter consisting of three 50:50 couplers to construct a TDM-PON with four branches and the feeder fiber is a 6-km single-mode fiber. The interference between communication and monitoring signals can be avoided by using a probe wavelength different from the communication wavelength. We did not introduce the optical line terminal into the experiment for the sake of convenience. In this case, all the FBGs can be replaced by fiber mirrors. The four reflectors with 90% reflectivity are placed in the corresponding branches at about 9, 10, 12 and 12.5 m after the power splitter. A distributed feedback laser diode without any isolator operating at 1550 nm is utilized as the probe laser. The laser is biased at 1.6 times the threshold current and has an output power of 2.0 mW. Through an optical coupler, 99% of the light is injected into the TDM-PON, and 1% is used for analysis. A photodetector with a 12-GHz bandwidth (Newport 1544B), a real-time oscilloscope with a 36-GHz bandwidth (LeCory LabMaster 10–36 Zi) and a radio-frequency spectrum analyzer with a 26.5-GHz bandwidth (Agilent N9020A) are used to record the output of the probe laser.

First, we measure the healthy PON and use the result as a reference, which we suggest should be implemented when the fiber network is installed. As shown in Fig. 3(a), the output intensity of the probe laser changes from a noisy stable state (gray) into a chaotic state (blue) with a larger fluctuation due to the feedback from the characteristic reflectors. The power spectrum of the chaotic signal is plotted in Fig. 3(b), illustrating a much stronger power than the noise and a wide bandwidth of chaos signal. Fig. 3(c) shows the ACF trace of the chaotic intensity waveform and the maximum value is normalized. Four correlation peaks at 6073.341, 6074. 590, 6076.023, and 6076.330 m are clearly identified and used to mark the corresponding branches. The tiny peaks around them are caused by the oscillation between each reflector, and the distinct level of the main peak is influenced by the slightly different feedback strength from each reflector. We ignore these tiny peaks and the main peak's distinct level because they have no role in our monitoring method. Since the distance between the reflector and the ONU in the real PON is small, we can ignore it and regard the marking peaks in ACF as the ONUs' contribution.

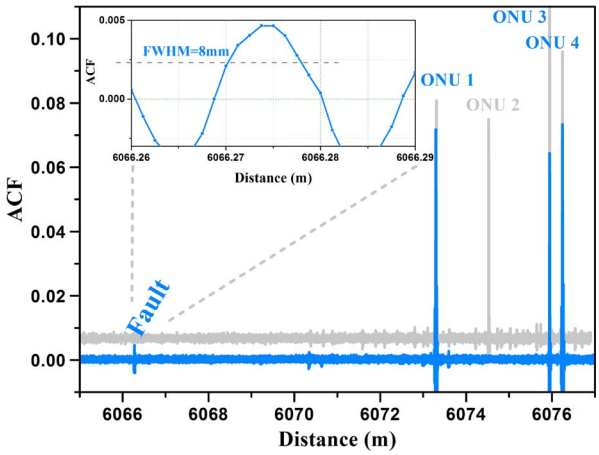

Fig. 4. Experiment result (blue) of the fault occurs in branch 2. The gray curve is the ACF of the healthy PON (see Fig. 3(c)) for the monitoring comparison. The disappeared peak (ONU 2) indicates the fault branch and the emerged peak reflects the fault position. The inset one is the magnification of the fault peak to analyze the spatial resolution.

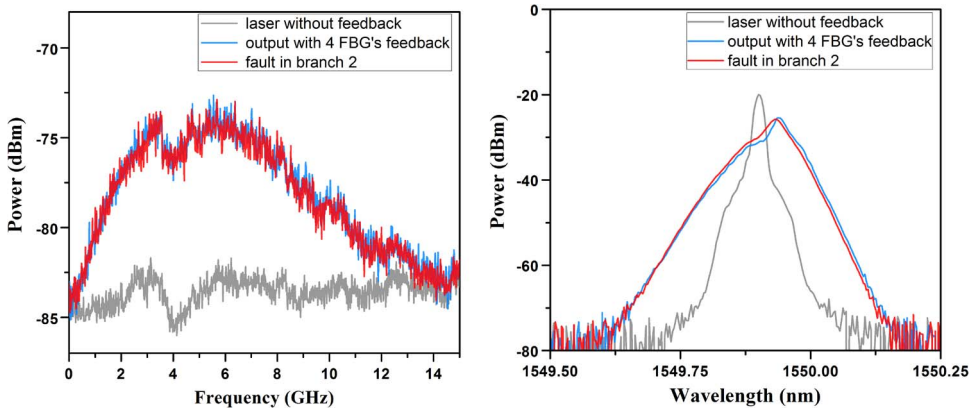

Fig. 5. Radio-frequency spectrum and optical spectral of the chaotic signal with or without fault occurs in branch 2.

We emulated a breakpoint by using an open connector at the beginning of branch 2. In this case, the feedback to the probe laser comes from the reflection of the breakpoint and the marking reflectors in other branches. Fig. 4 plots the corresponding ACF trace. By comparing it with the reference trace (gray line), one can find that the second marking peak disappears and another short peak appears at 6066.274 m. This means that both the fault and the corresponding branch are identified. Furthermore, the spatial resolution is estimated by the full-width-at-half-maximum (FWHM) of the correlation peak. The inset in Fig. 4 plots the magnified correlation peaks of the fault. It is found that the FWHM of the correlation peak is 8 mm which relates to the bandwidth of the chaos [51]. If the fault occurs in the feeder fiber, there is only feedback from reflection of the breakpoint. All peaks marking branches will disappear and a new peak will emerge between the operator and these marking peaks. This correlation peak corresponds to the external cavity signature of the fault feedback. We remark that it is hard to differentiate faults whose distances are within a small range of 8 mm, i.e. the spatial resolution, due to the overlap of correlation peaks, while the probability of the occurrence of overlap is very low.

Finally, we demonstrate the radio-frequency spectrum and optical spectral of the chaotic laser with or without fault occurs. Note that the fault occurs in branch 2 and the optical spectra are measured by an optical spectrum analyzer with a resolution bandwidth of 0.02 nm (YOKOGAWA AQ6370C). As shown in Fig. 5, the gray curves are the laser output with no

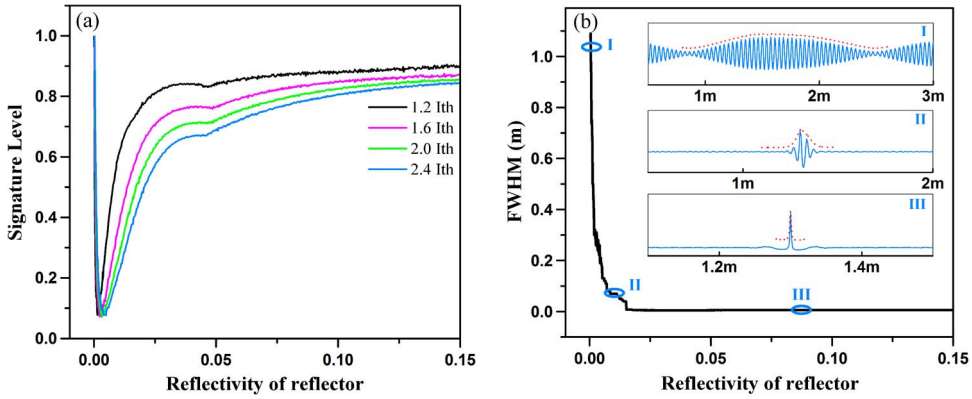

Fig. 6. (a) Level and (b) FWHM of the external cavity signature in ACF of the chaotic laser versus the reflectivity of reflector.

feedback, blue curves are the chaotic laser with four FBG's feedback, and the red curves are the chaotic laser when fault occurs in branch 2. Obviously, there is no significant difference on the spectra before and after the fault occurs.

4. Discussion

It should be recalled from extensive previous work that the state of the chaos is closely related to the strength of the optical feedback. Moreover, the characteristic of the external cavity signature in ACF can be influenced by the chaos state. Therefore, we utilize a theoretical model based on the Lang-Kobayashi rate equations [67] to analyze the relationship between the signature in the ACF curve and the reflectivity of the reflector. The intrinsic parameters of the laser are taken from Ref. [42] and the reflector sites at 1.3 m with the reflectivity changing from 0.00001 to 0.15. The sampling rate is set as 80 GS/s. As shown in Fig. 6(a), we demonstrate the evolution of the signature's level. The level first decreases rapidly to the lowest point and then rises slowly to a stable value which is consistent with the previous research [61], [68]. The reflectivity at the inflection point, i.e. the lowest signature-level point, is about 0.0012, which indicates the emergence of strong chaos [69], [70]. We set bias currents at 1.2, 1.6, 2.0 and 2.4 times the laser threshold current to analyze and acquire similar results. It should be point out that the signature is still identified when the reflectivity is 0.00001. This reflectivity evaluates the measurable length of a fiber link. Assuming the reflection level of a fault is –20 dB, and total insertion loss is –5 dB, the method can afford a fiber round-trip loss of 25 dB. Considering the fiber loss coefficient is 0.2 dB/km, the monitoring fiber length can reach 62.5 km. For the splitting number, 25 dB can afford 16 branches.

Furthermore, we illustrate the FWHM of the ACF in the state of the laser for alternate reflection, as shown in Fig. 6(b). Due to the similar overall behavior for the different currents in Fig. 6(a), we only plot the variation curve with 1.6 times at threshold current. The inset figures show the magnified ACF curve at the position corresponding to the external reflector. In the situation with low reflectivity, the wide oscillated curve makes the peak diverge from the accurate position. The FWHM of the wide oscillated peaks is estimated by the envelope, colored in red. We find that the maximum FWHM is just 1.1 m, which can satisfy the demands of standard monitoring, and decreases rapidly to the stable value of 2 mm.

For chaos generation with multiple reflectors, there are multiple sets of external-cavity modes. These modes have a slight gain competition (the laser mode gets most of the gain) in laser cavity and thus affect each other slightly. We believe that this effect has no influence on our measurement of fiber faults in general. The reason is that the fiber fault is identified by the disappearance of the marking correlation peak and the appearance of the fault-induced signature peak. The appearance or disappearance of signature peak is only determined by whether the fault exists or not.

It should be pointed out that the radio-frequency spectrum analyzer and optical spectrum analyzer are not required for measurement. The high-performance scope is just used to record the time series of the chaotic signal and it can be replaced by a data acquisition card. According to our previous results in [51], a data acquisition card with 3–4 GHz bandwidth is sufficient for a spatial resolution of about 1 cm.

In addition, the present experiment can only capture the reflective events which can induce chaos in the monitoring laser. Dynamic range and high spatial resolution can be increased by the amplification of the laser light. While similar to the other techniques in TDM-PON monitoring, we cannot distinguish and locate multi-faults at the same time. These challenges remain to be studied further.

5. Conclusion

In conclusion, we propose and experimentally demonstrate a technique for fiber fault monitoring in TDM-PON by utilizing the external cavity signature of a semiconductor laser with optical feedback. The FBGs in each branch provide the optical feedback to the laser, which then becomes a chaos generation system with multi-feedback. According to the appearance and disappearance of cavity length signatures, we can distinguish the faulty branch and locate the fault point simultaneously. The experimental results demonstrate the feasibility of our concept, and the spatial resolution is decreased to 8 mm compared with the meters resolution in [33]. This method combines the subjects of the nonlinear dynamic laser and the TDM-PON monitoring, and lots of works is worth deep-going researching. We believe that the simple structure with one semiconductor laser and same FBGs can dramatically decrease the operational expenditure and be worthy of further attention.

Acknowledgment

The authors would like to thank Prof. K. A. Shore and T. C. Scott for helping in the preparation of this document. T. C. Scott is supported in China by the project GDW201400042 for the "High-end Foreign Experts Project."

References

[1] M. A. Esmail and H. Fathallah, "Physical layer monitoring technique for TDM-passive optical networks: A survey," *IEEE Commun. Surveys Tuts.*, vol. 15, no. 2, pp. 943–958, 2nd Quart. 2013.
[2] M. M. Rad, K. Fouli, H. A. Fathallah, L. A. Rusch, and M. Maier, "Passive optical network monitoring: Challenges and requirements," *IEEE Commun. Mag.*, vol. 49, no. 2, pp. S45–S52, Feb. 2011.
[3] K. Yuksel, V. Moeyaert, M. Wuilpart, and P. Megret, "Optical layer monitoring in passive optical networks (PONs): A review," in *Proc. 10th Anniv. ICTON*, Athens, Greece, 2008, pp. 92–98.
[4] P. J. Urban and S. Dahlfort, "OTM- and OTDR-based cost-efficient fiber fault identification and localization in passive optical network," in *Proc. Opt. Fiber Commun. Conf.*, Los Angeles, CA, USA, 2011, pp. 1–3.
[5] N. B. Chuan, A. Premadi, M. S. Ab-Rahman, and K. Jumari, "Physical layer monitoring in 8-branched PON-based i-FTTH," in *Proc. IEEE ICP*, Langkawi, Malaysia, 2010, pp. 1–5.
[6] J. H. Lee, K. M. Choi, J. H. Moon, and C. H. Lee, "A remotely reconfigurable PON architecture for efficient maintenance and protection," in *Proc. IEEE OFC NFOEC*, San Diego, CA, USA, 2009, pp. 1–3.
[7] M. S. Ab-Rahman, B. C. Ng, A. Premadi, and K. Jumari, "Transmission surveillance and self-restoration against fibre fault for time division multiplexing using passive optical network," *IET Commun.*, vol. 3, no. 12, pp. 1896–1906, Dec. 2009.
[8] N. Nakao *et al.,* "Maintenance method using 1650-nm wavelength band for optical fiber cable networks," *J. Lightw. Technol.*, vol. 19, no. 10, pp. 1513–1520, Oct. 2001.
[9] T. Ebihara, N. Nakao, and M. Kuroiwa, "Novel automatic remote fiber line testing system and new fiber termination module for expanding local subscriber loops," in *Proc. IEEE 22nd ECOC*, Oslo, Norway, 1996, pp. 39–42.
[10] C. Y. Kuang and C. Sien, "Fault-locating and supervisory technique for multistaged branched optical networks," *IEEE Photon. Technol. Lett.*, vol. 6, no. 7, pp. 876–879, Jul. 1994.
[11] N. Tomita *et al.,* "Design and performance of a novel automatic fiber line testing system with OTDR for optical subscriber loops," *J. Lightw. Technol.*, vol. 12, no. 5, pp. 717–726, May 1994.
[12] M. Simard, "OTDR PON testing: The challenges—The solution," *Application Note 201*, 2009.
[13] J. Hehmann and T. Pfeiffer, "New monitoring concepts for optical access networks," *Bell Labs Tech. J.*, vol. 13, no. 1, pp. 183–198, Spring 2008.

[14] C. Wei *et al.,* "A novel technique for low-cost embedded non-intrusive fiber monitoring of P2MP optical access networks," in *Proc. Opt. Fiber Commun. Conf. Expo. Nat. Fiber Opt. Eng. Conf.*, Anaheim, CA, USA, 2007, pp. 1–3.
[15] B. De Mulder, C. Wei, J. Bauwelinck, J. Vandewege, and Q. X. Zhi, "Nonintrusive fiber monitoring of TDM optical networks," *J. Lightw. Technol.*, vol. 25, no. 1, pp. 305–317, Jan. 2007.
[16] H. Schmuck, J. Hehmann, M. Straub, and T. Pfeiffer, "Embedded OTDR techniques for cost-efficient fibre monitoring in optical access networks," in *Proc. IEEE ECOC*, Cannes, France, 2006, pp. 1–2.
[17] W. Chen, B. De Mulder, J. Vandewege, and X. Qiu, "Embedded OTDR monitoring of the fiber plant behind the PON power splitter," in *Proc. IEEE Symp. LEOS*, Eindhoven, The Netherlands, 2006, pp. 13–16.
[18] F. Caviglia and V. C. Di. Biase, "Optical maintenance in PONs," in *Proc. 24th Eur. Conf. Opt. Commun.*, Madrid, Spain, 1998, pp. 621–625.
[19] C. K. Chan, F. Tong, L. K. Chen, J. Song, and D. Lam, "A practical passive surveillance scheme for optically amplified passive branched optical networks," *IEEE Photon. Technol. Lett.*, vol. 9, no. 4, pp. 526–528, Apr. 1997.
[20] U. Hilbk *et al.,* "Selective OTDR measurements at the central office of individual fiber links in a PON," in *Proc. IEEE Conf. OFC*, Dallas, TX, USA, 1997, p. 1.
[21] C. K. Chan, F. Tong, L. K. Chen, K. P. Ho, and D. Lam, "Fiber-fault identification for branched access networks using a wavelength-sweeping monitoring source," *IEEE Photon. Technol. Lett.*, vol. 11, no. 5, pp. 614–616, May 1999.
[22] C. H. Yeh and S. Chi, "Optical fiber-fault surveillance for passive optical networks in S-band operation window," *Opt. Exp.*, vol. 13, no. 14, pp. 5494–5498, Jul. 2005.
[23] W. Shin, B. A. Yu, Y. L. Lee, T. J. Eom, and Y. C. Noh, "Flexible fiber fault detecting technique based on wavelength swept fiber laser for passive optical network," in *Proc. CLEO/PACIFIC RIM*, Shanghai, China, 2009, pp. 1–2.
[24] K. Tanaka, M. Tateda, and Y. Inoue, "Measuring the individual attenuation distribution of passive branched optical networks," *IEEE Photon. Technol. Lett.*, vol. 8, no. 7, pp. 915–917, Jul. 1996.
[25] N. I. M. Rawi, F. Abdullah, M. Z. Jamaludin, and M. H. Al-Mansoori, "Live monitoring system for Ethernet passive optical network health using fiber Bragg grating," in *Proc. IEEE SCOReD*, 2010, pp. 56–58.
[26] H. Fathallah and L. A. Rusch, "Code-division multiplexing for in-service out-of-band monitoring of live FTTH-PONs," *J. Opt. Netw.*, vol. 6, no. 7, pp. 819–829, 2007.
[27] S. C. Ko, S. C. Lin, and Y. H. Huang, "A fiber fault monitoring design for PON system using reflective signal," in *Proc. 16th OECC*, Kaohsiung, Taiwan, 2011, pp. 555–556.
[28] X. Long, C. Xiaofei, X. Zhaowen, and H. Qirui, "Lengthened simplex codes with complementary correlation for faulty branch detection in TDM-PON," *IEEE Photon. Technol. Lett.*, vol. 25, no. 23, pp. 2315–2318, Dec. 2013.
[29] N. Honda, D. Iida, H. Izumita, and Y. Azuma, "In-service line monitoring system in PONs using 1650-nm Brillouin OTDR and fibers with individually assigned BFSs," *J. Lightw. Technol.*, vol. 27, no. 20, pp. 4575–4582, Oct. 2009.
[30] K. Yuksel, M. Wuilpart, V. Moeyaert, and P. Megret, "Optical frequency domain reflectometry: A review," in *Proc. 11th ICTON*, Azores, Portugal, 2009, pp. 1–5.
[31] K. Yuksel, M. Wuilpart, V. Moeyaert, and P. Megret, "Novel monitoring technique for passive optical networks based on optical frequency domain reflectometry and fiber Bragg gratings," *J. Opt. Commun. Netw.*, vol. 2, no. 7, pp. 463–468, Jul. 2010.
[32] M. Thollabandi, H. Bang, K. W. Shim, S. Hann, and C. S. Park, "An optical surveillance technique based on cavity mode analysis of SL-RSOA for GPON," *Opt. Fiber Technol.*, vol. 15, no. 5/6, pp. 451–455, Oct.–Dec. 2009.
[33] P. J. Urban, G. Vall-Llosera, E. Medeiros, and S. Dahlfort, "Fiber plant manager: An OTDR-and OTM-based PON monitoring system," *IEEE Commun. Mag.*, vol. 51, no. 2, pp. S9–S15, Feb. 2013.
[34] J. Park, J. Baik, and C. Lee, "Fault-detection technique in a WDM-PON," *Opt. Exp.*, vol. 15, no. 4, pp. 1461–1466, Feb. 2007.
[35] M. Legre, R. Thew, H. Zbinden, and N. Gisin, "High resolution optical time domain reflectometer based on 1.55 μm up-conversion photon-counting module," *Opt. Exp.*, vol. 15, no. 13, pp. 8237–8242, 2007.
[36] S. Wielandy, M. Fishteyn, and B. Zhu, "Optical performance monitoring using nonlinear detection," *J. Lightw. Technol.*, vol. 22, no. 3, pp. 784–793, Mar. 2004.
[37] M. Zoboli and P. Bassi, "High spatial resolution OTDR attenuation measurements by a correlation technique," *Appl. Opt.*, vol. 22, no. 23, pp. 3680–3681, Dec. 1983.
[38] H. K. Shim, K. Y. Cho, Y. Takushima, and Y. C. Chung, "Correlation-based OTDR for in-service monitoring of 64-split TDM PON," *Opt. Exp.*, vol. 20, no. 5, pp. 4921–4926, Dec. 2012.
[39] T. Zhao *et al.,* "Fiber fault location utilizing traffic signal in optical network," *Opt. Exp.*, vol. 21, no. 20, pp. 23978–23984, Oct. 2013.
[40] Y. Takushima and Y. C. Chung, "Optical reflectometry based on correlation detection and its application to the in-service monitoring of WDM passive optical network," *Opt. Exp.*, vol. 15, no. 9, pp. 5318–5326, 2007.
[41] F. Y. Lin and J. M. Liu, "Ambiguity functions of laser-based chaotic radar," *IEEE J. Quant. Electron.*, vol. 40, no. 12, pp. 1732–1738, Dec. 2004.
[42] A. Wang, B. Wang, L. Li, Y. Wang, and K. A. Shore, "Optical heterodyne generation of high-dimensional and broadband white chaos," *IEEE J. Sel. Topics. Quantum Electron.*, vol. 21, no. 6, pp. 1–10, Nov./Dec. 2015.
[43] Y. H. Hong, P. S. Spencer, and K. A. Shore, "Wideband chaos with time-delay concealment in vertical-cavity surface-emitting lasers with optical feedback and injection," *IEEE J. Quantum Electron.*, vol. 50, no. 4, pp. 236–242, Apr. 2014.
[44] A. B. Wang *et al.,* "Generation of wideband chaos with suppressed time-delay signature by delayed self-interference," *Opt. Exp.*, vol. 21, no. 7, pp. 8701–8710, Apr. 2013.
[45] Y. H. Hong, X. F. Chen, P. S. Spencer, and K. A. Shore, "Enhanced flat broadband optical chaos using low-cost VCSEL and fiber ring resonator," *IEEE J. Quantum Electron.*, vol. 51, no. 3, pp. 1–6, Mar. 2015.
[46] A. B. Wang *et al.,* "Generation of flat-spectrum wideband chaos by fiber ring resonator," *Appl. Phys. Lett.*, vol. 102, no. 3, 2013, Art. ID 031112.
[47] Y. C. Wang, B. J. Wang, and A. B. Wang, "Chaotic correlation optical time domain reflectometer utilizing laser diode," *IEEE Photon. Technol. Lett.*, vol. 20, no. 19, pp. 1636–1638, Oct. 2008.

[48] M. J. Zhang *et al.,* "Remote radar based on chaos generation and radio over fiber," *IEEE Photon. J.*, vol. 6, no. 5, pp. 1–12, Oct. 2014.
[49] F. Y. Lin and J. M. Liu, "Chaotic lidar," *IEEE J. Sel. Top. Quantum Electron.*, vol. 10, no. 5, pp. 991–997, Sep./Oct. 2004.
[50] K. Myneni, T. A. Barr, B. R. Reed, S. D. Pethel, and N. J. Corron, "High-precision ranging using a chaotic laser pulse train," *Appl. Phys. Lett.*, vol. 78, no. 11, pp. 1496–1498, 2001.
[51] A. B. Wang *et al.,* "Precise fault location in WDM-PON by utilizing wavelength tunable chaotic laser," *J. Lightw. Technol.*, vol. 30, no. 21, pp. 3420–3426, 2012.
[52] J. Mork, B. Tromborg, and J. Mark, "Chaos in semiconductor lasers with optical feedback: Theory and experiment," *IEEE J. Quantum Electron.*, vol. 28, no. 1, pp. 93–108, Jan. 1992.
[53] J. Mork, J. Mark, and B. Tromborg, "Route to chaos and competition between relaxation oscillations for a semiconductor laser with optical feedback," *Phys. Rev. Lett.*, vol. 65, no. 16, pp. 1999–2002, Oct. 1990.
[54] T. Mukai and K. Otsuka, "New route to optical chaos: Successive-subharmonic-oscillation cascade in a semiconductor laser coupled to an external cavity," *Phys. Rev. Lett.*, vol. 55, no. 17, pp. 1711–1714, Oct. 1985.
[55] M. Sciamanna and K. A. Shore, "Physics and applications of laser diode chaos," *Nature Photon.*, vol. 9, no. 3, pp. 151–162, 2015.
[56] M. C. Soriano, J. Garcia-Ojalvo, C. R. Mirasso, and I. Fischer, "Complex photonics: Dynamics and applications of delay-coupled semiconductors lasers," *Rev. Mod. Phys.*, vol. 85, no. 1, pp. 421–470, Jan.–Mar. 2013.
[57] D. Rontani, A. Locquet, M. Sciamanna, and D. S. Citrin, "Loss of time-delay signature in the chaotic output of a semiconductor laser with optical feedback," *Opt. Lett.*, vol. 32, no. 20, pp. 2960–2962, Oct. 2007.
[58] D. Rontani, A. Locquet, M. Sciamanna, D. S. Citrin, and S. Ortin, "Time-delay identification in a chaotic semiconductor laser with optical feedback: A dynamical point of view," *IEEE J. Quantum Electron.*, vol. 45, no. 7, pp. 879–1891, Jul. 2009.
[59] Y. Wu, Y. C. Wang, P. Li, A. B. Wang, and M. J. Zhang, "Can fixed time delay signature be concealed in chaotic semiconductor laser with optical feedback?" *IEEE J. Quantum Electron.*, vol. 48, no. 11, pp. 1371–1379, Nov. 2012.
[60] J. P. Toomey and D. M. Kane, "Mapping the dynamic complexity of a semiconductor laser with optical feedback using permutation entropy," *Opt. Exp.*, vol. 22, no. 2, pp. 1713–1725, Jan. 2014.
[61] J. G. Wu, G. Q. Xia, and Z. M. Wu, "Suppression of time delay signatures of chaotic output in a semiconductor laser with double optical feedback," *Opt. Exp.*, vol. 17, no. 22, pp. 20124–20133, 2009.
[62] Z. Q. Zhong, Z. M. Wu, J. G. Wu, and G. Q. Xia, "Time-delay signature suppression of polarization-resolved chaos outputs from two mutually coupled VCSELs," *IEEE Photon. J.*, vol. 5, no. 2, Apr. 2013, Art. ID 1500409.
[63] S. Y. Xiang *et al.,* "Quantifying chaotic unpredictability of vertical-cavity surface-emitting lasers with polarized optical feedback via permutation entropy," *IEEE J. Sel. Topics Quantum Electron.*, vol. 17, no. 5, pp. 1212–1219, Sep./Oct. 2011.
[64] N. Oliver, M. C. Soriano, D. W. Sukow, and I. Fischer, "Dynamics of a semiconductor laser with polarization-rotated feedback and its utilization for random bit generation," *Opt. Lett.*, vol. 36, no. 23, pp. 4632–4634, Dec. 2011.
[65] S. Priyadarshi, Y. Hong, I. Pierce, and K. A. Shore, "Experimental investigations of time-delay signature concealment in chaotic external cavity VCSELs subject to variable optical polarization angle of feedback," *IEEE J. Sel. Top. Quantum Electron.*, vol. 19, no. 4, Jul./Aug. 2013, Art. ID 1700707.
[66] S. S. Li, Q. Liu, and S. C. Chan, "Distributed feedbacks for time-delay signature suppression of chaos generated from a semiconductor laser," *IEEE Photon. J.*, vol. 4, no. 5, pp. 1930–1935, Oct. 2012.
[67] R. Lang and K. Kobayashi, "External optical feedback effects on semiconductor injection laser properties," *IEEE J. Quantum Electron.*, vol. QE-16, no. 3, pp. 347–355, Mar. 1980.
[68] X. Porte *et al.,* "Autocorrelation properties of chaotic delay dynamical systems: A study on semiconductor lasers," *Phys. Rev. E, Stat. Phys. Plasmas Fluids Relat. Interdiscip. Top.*, vol. 90, no. 5, Nov. 2014, Art. ID 052911.
[69] S. Heiligenthal *et al.,* "Strong and weak chaos in networks of semiconductor lasers with time-delayed couplings," *Phys. Rev. E, Stat. Phys. Plasmas Fluids Relat. Interdiscip. Top.*, vol. 88, no. 1, Jul. 2013, Art. ID 012902.
[70] X. Porte, M. C. Soriano, and I. Fischer, "Similarity properties in the dynamics of delayed-feedback semiconductor lasers," *Phys. Rev. A, Gen. Phys.*, vol. 89, no. 2, Feb. 2014, Art. ID 023822.